Zero-offset seismic amplitude decomposition and migration

Bjørn Ursin, Norwegian University of Science and Technology (NTNU), Norway

Martin Tygel, State University of Campinas (UNICAMP), Brazil

Abstract

In an anisotropic medium, a normal-incidence wave is multiply transmitted and reflected down to a reflector where the phase velocity vector is parallel to the interface normal. The ray code of the up-going wave is equal to the ray code of the down-going wave in reverse order. The geometrical spreading, KMAH index and transmission and reflection coefficients of the normal-incidence ray can be simply expressed in terms of products or sums of the corresponding quantities of the one-way normal and NIP waves. Here we show that the amplitude of the ray-theoretic Green's function for the reflected wave also follow a similar decomposition in terms of the amplitude of the Green's function of the NIP wave and the normal wave. We use this property to propose three schemes for true-amplitude post-stack depth migration in anisotropic media where the image represents an estimate of the zero-offset reflection coefficient. The first is a map migration procedure in which selected primary zero-offset reflections are converted into depth with attached true amplitudes. The second is a ray-based, Kirchhoff type full migration. Finally, a wave equation continuation algorithm can be used to reverse-propagate the recorded wavefield in a half-velocity model with half the elastic constants and double the density. The image is formed by taking the reverse-propagated wavefield at time equal zero followed by a geometrical spreading correction.

Introduction

A stacked seismic section is considered as an approximation of a zero-offset seismic section. Each trace is the result of a seismic experiment where the source and receiver are located at the same surface point. In the following, we restrict our considerations to zero-offset reflections that can be formulated as normal incidence rays, namely, each of them reflects at a normal incidence point (NIP) and returns to the source/receiver point following the same path. In anisotropic media this can occur when the slowness vector is parallel to the surface normal at the NIP interface. For a multiple transmitted, reflected and converted wave this requires that the ray code up is the ray code down in reverse order. This includes the PP and SS primary reflections, but not the PS converted wave reflection.

A stacked section is obtained by summing the traces in a common-midpoint gather after they have been corrected for normal moveout (NMO). This requires the knowledge of the NMO or stacking velocity which for 3-D data are given by a 2×2 symmetric matrix (Ursin, 1982). Krey (1976) and Chernyak and Gritsenko (1979) showed that this NMO velocity matrix can be computed from the curvature of a fictitious one-way wave that starts as a point source at the NIP reflection point. This wave was called the *NIP wave* by Hubral (1983).

For the purpose of migrating stacked data, Loewenthal et al. (1976) introduced the exploding reflector model for zero-offset primary reflections. This is another fictitious experiment conducted in a fictitious medium with half the velocity of the true medium. The sources are placed along the reflector, and all sources are activated at the same time set equal to zero. An equivalent description of the exploding reflector model is that, in the vicinity of each point of the reflector, a wave front with the same shape as the reflector starts its way up and is recorded at the surface. This one-way wave has been called the *normal wave* by Hubral (1983). Iversen (2006) gave a complete review of normal incidence reflections with many new results. While Hubral (1983) considered wavefront curvature in an isotropic medium, Iversen (2006) considered Green's functions in anisotropic elastic media for PP and SS primary reflections expressed by asymptotic ray theory. In particular, he obtained results for the relative geometrical spreading and the KMAH index for the normal-incidence reflected wave, the NIP wave and the normal wave.

In this paper we have three objectives. The first is to simplify Iversen's results by using flux-normalized reflection and transmission coefficients instead of amplitude-normalized ones. As a consequence, the product of the reflection and transmission coefficients for the down-going wave is equal to the corresponding product for the up-going wave (Chapman, 1994). From this it follows that the geometric ray approximation of the Green's tensor of the normal-incidence reflected ray can be expressed in terms of Greens's tensor of the reverse NIP wave and the tensor response of the normal wave. We also compare this decomposition to the standard decomposition of the geometrical spreading and KMAH index at the reflecting interface (Schleicher et al., 2001).

Map migration (Kleyn, 1977) is the transformation of a two-way normal-incidence traveltime map into a reflecting interface at depth, given the smooth parameters of the elastic medium. Gjøystdal and Ursin (1981) extended this to also estimating the medium parameters, given non-zero offset traveltimes or stacking velocities. Gjøystdal et al. (1984) proposed to use the normal wave to downward continue the curvature of the zero-offset reflection to obtain the curvature of the interface. Our second objective is to estimate the zero-offset reflection coefficient. By dynamic ray tracing along normal-incidence rays, we compute amplitude corrections which can be applied to the recorded amplitudes to obtain an estimate of the normal-incidence reflection coefficient at the depth interface.

True-amplitude post-stack migration in an isotropic medium can be done by ray-based, Kirchhoff diffraction stack algorithm with simple weights (Schleicher et al., 1993). We give a new formula for post-stack in anisotropic media using results from Ursin (2004).

Post-stack depth migration in an isotropic or anisotropic medium is also done downward continuation of the recorded data in a model with half the medium velocity (Loewenthal, 1976; Gazdag and Sguazzero, 1984). An estimate of the reflectivity is then obtained from the reverse-propagated wavefield at time equal zero. In the Appendix we show how to extend this scheme to anisotropic media by using elastic parameters divided by two and density multiplied by two. This will half the phase and group velocities of the medium. This downward continuation corresponds to downward continuation of the normal wave, except for the doubling of the traveltime. Therefore, there is an uncompensated part of the geometrical spreading, which remains in the amplitude of the migrated image. Our third objective is to estimate this residual geometrical spreading correction. Following the lines in Bleistein (1987) and Tygel et al. (1993), this can be obtained by upon the use of a second Kirchhoff zero-offset migration with a different weight.

Decomposition of Normal-Incidence Reflections

We consider an anisotropic elastic medium with a multiple transmitted, reflected and converted wave which starts at a source point, $\mathbf{x}$, at the surface and is reflected back at a point $\mathbf{y}$ at an interface with the slowness or phase velocity parallel to the interface normal, and such that the ray code for the up-going wave is the wave code for the down-going wave in reverse order. Such wave, referred here as *normal-incidence reflected wave*, comes back to the source point $\mathbf{x}$, which is a zero-offset point, see Figure 1. Note that for heterogeneous media, even isotropic, one can conceive reflected waves with coincident source/receiver position which have not been reflected at normal incidence. Reversing the direction of the incident leg, this would be the situation of a multi-arrival path from the reflection point to the coincident source-receiver point. Such waves are not considered here.

In the following, we will work in the frequency domain. It is instructive to introduce a few definitions. For any given real trace, $u_R(\mathbf{x},t)$, at trace location, $\mathbf{x}$, and time, t, we consider the Fourier transform pair (see, e.g., Červený, 2001, Appendix)

$$U_R(\mathbf{x},\omega) = \int_{-\infty}^{\infty} u_R(\mathbf{x},t)\, e^{i\omega t}\, dt \tag{1}$$

and

$$u_R(\mathbf{x},t) = Re\left\{ \frac{1}{\pi} \int_0^{\infty} U_R(\mathbf{x},\omega)\, e^{-i\omega t}\, d\omega \right\} . \tag{2}$$

The geometric ray approximation of the Green's function for the reflected ray is, in the frequency domain, proportional to the scalar response function (see the next section)

$$U_R(\mathbf{x},\mathbf{y},\mathbf{x};\omega) = \frac{e^{-i\frac{\pi}{2}\kappa_R}\, e^{i\omega T_R}}{\mathscr{L}_R}\, t_U\, r_N\, t_D\, . \tag{3}$$

In the above equation, ω is the circular frequency, $T_R = T_R(\mathbf{x},\mathbf{y},\mathbf{x})$ is the two-way traveltime, $\kappa_R = \kappa_R(\mathbf{x},\mathbf{y},\mathbf{x})$ is the KMAH index, $r_N = r_N(\mathbf{y})$ is the normal-incidence reflection coefficient at the reflection point NIP and $t_D = t_D(\mathbf{y},\mathbf{x})$ and $t_U = t_U(\mathbf{x},\mathbf{y})$ are the product of the transmission and reflection coefficients for the wave going up and down, respectively. All the reflection and transmission coefficients are normalized with respect to the energy flux normal to each interface, and then the coefficients are reciprocal (Chapman, 1994), so that

$$t_D = \Pi t_{Dk} = \Pi t_{Uk} = t_U\, . \tag{4}$$

The relative geometrical spreading is

$$\mathscr{L}_R = \mathscr{L}_R(\mathbf{x},\mathbf{y},\mathbf{x}) = |\det \mathbf{Q}_2(\mathbf{x},\mathbf{y},\mathbf{x})|^{1/2}\, , \tag{5}$$

where the 2×2 matrix $\mathbf{Q}_2(\mathbf{x},\mathbf{y},\mathbf{x})$ is part of the two-way 4×4 ray propagator matrix (Červený, 2001; Chapman, 2004)

$$\underline{\Pi}(\mathbf{x},\mathbf{y},\mathbf{x}) = \begin{pmatrix} \mathbf{Q}_1(\mathbf{x},\mathbf{y},\mathbf{x}) & \mathbf{Q}_2(\mathbf{x},\mathbf{y},\mathbf{x}) \\ \mathbf{P}_1(\mathbf{x},\mathbf{y},\mathbf{x}) & \mathbf{P}_2(\mathbf{x},\mathbf{y},\mathbf{x}) \end{pmatrix} . \tag{6}$$

The reflected wave is schematically shown in Figure 2.

The NIP wave is a hypothetical wave that starts as a point source of unit amplitude at the normal-incidence point and propagates within the original medium towards the given zero-offset surface location where it is recorded, see Figure 3. The response function is (see equation 3)

$$U_{NIP}(\mathbf{x},\mathbf{y};\omega) = \frac{e^{-i\frac{\pi}{2}\kappa_{NIP}}\, e^{i\omega T_R/2}}{\mathscr{L}_{NIP}}\, t_U\, , \tag{7}$$

where the relative geometrical spreading factor, $\mathscr{L}_{NIP} = |\det \mathbf{Q}_{NIP}(\mathbf{x},\mathbf{y})|^{1/2}$, is computed from

$$\begin{pmatrix} \mathbf{Q}_{NIP}(\mathbf{x},\mathbf{y}) \\ \mathbf{P}_{NIP}(\mathbf{x},\mathbf{y}) \end{pmatrix} = \begin{pmatrix} \mathbf{Q}_1(\mathbf{x},\mathbf{y}) & \mathbf{Q}_2(\mathbf{x},\mathbf{y}) \\ \mathbf{P}_1(\mathbf{x},\mathbf{y}) & \mathbf{P}_2(\mathbf{x},\mathbf{y}) \end{pmatrix} \begin{pmatrix} \mathbf{O} \\ \mathbf{I} \end{pmatrix} = \begin{pmatrix} \mathbf{Q}_2(\mathbf{x},\mathbf{y}) \\ \mathbf{P}_2(\mathbf{x},\mathbf{y}) \end{pmatrix} \tag{8}$$

and $\kappa_{NIP} = \kappa_{NIP}(\mathbf{x},\mathbf{y})$ is the KMAH index for the NIP wave. Here, the one-way upward ray propagator matrix (Červený, 2001; Chapman, 2004) is

$$\underline{\Pi}(\mathbf{x},\mathbf{y}) = \begin{pmatrix} \mathbf{Q}_1(\mathbf{x},\mathbf{y}) & \mathbf{Q}_2(\mathbf{x},\mathbf{y}) \\ \mathbf{P}_1(\mathbf{x},\mathbf{y}) & \mathbf{P}_2(\mathbf{x},\mathbf{y}) \end{pmatrix} . \tag{9}$$

A second hypothetical wave is the normal wave, which originates at the reflecting surface with a wavefront curvature of the interface at that point, see Figure 4.

We shall let the normal wave start with amplitude r_N, the normal-incidence reflection coefficient, so that the response function is

$$U_N(\mathbf{x},\mathbf{y};\omega) = \frac{e^{-i\frac{\pi}{2}\kappa_N}\, e^{i\omega T_R/2}}{\mathscr{L}_N}\, t_U\, r_N\, . \tag{10}$$

The geometrical spreading, $\mathscr{L}_N = |\det \mathbf{Q}_N(\mathbf{x},\mathbf{y})|^{1/2}$ is computed from

$$\begin{aligned} \begin{pmatrix} \mathbf{Q}_N(\mathbf{x},\mathbf{y}) \\ \mathbf{P}_N(\mathbf{x},\mathbf{y}) \end{pmatrix} &= \begin{pmatrix} \mathbf{Q}_1(\mathbf{x},\mathbf{y}) & \mathbf{Q}_2(\mathbf{x},\mathbf{y}) \\ \mathbf{P}_1(\mathbf{x},\mathbf{y}) & \mathbf{P}_2(\mathbf{x},\mathbf{y}) \end{pmatrix} \begin{pmatrix} \mathbf{I} \\ v^{-1}(\mathbf{y})\mathbf{D}(\mathbf{y}) \end{pmatrix} \\ &= \begin{pmatrix} \mathbf{Q}_1(\mathbf{x},\mathbf{y}) + v^{-1}(\mathbf{y})\mathbf{Q}_2(\mathbf{x},\mathbf{y})\mathbf{D}(\mathbf{y}) \\ \mathbf{P}_1(\mathbf{x},\mathbf{y}) + v^{-1}(\mathbf{y})\mathbf{P}_2(\mathbf{x},\mathbf{y})\mathbf{D}(\mathbf{y}) \end{pmatrix} , \end{aligned} \tag{11}$$

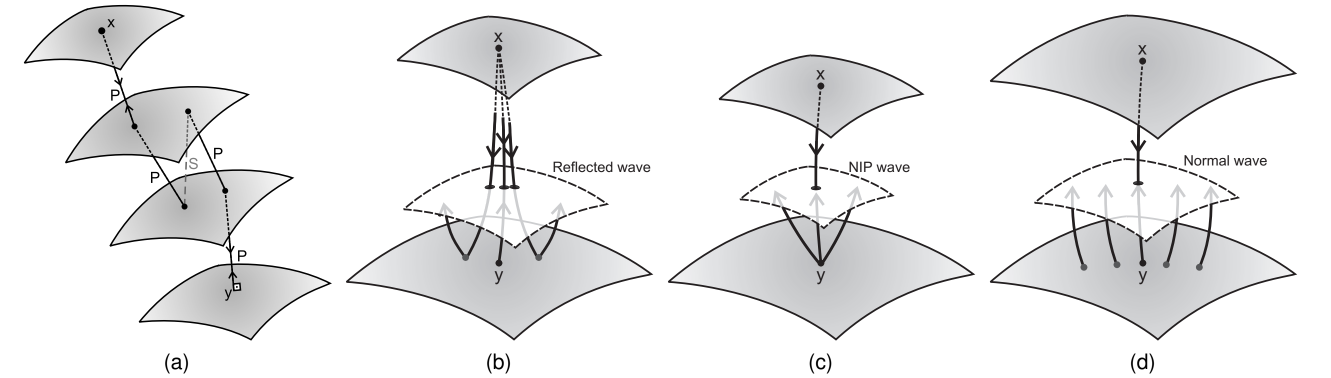

Figure 1: (a) The ray path of a multiple transmitted, reflected and converted NIP path; (b) The reflected wave from a point source, $\mathbf{x}$, at the measurement surface. Also shown is the normal-incident-point, $\mathbf{y}$, at the reflector; (c) The NIP wave starting at the normal-incidence point, $\mathbf{y}$, at the reflector and (d) The normal wave starting as wavefront that coincides with the reflector in the vicinity of the normal-incident-point, $\mathbf{y}$.

where $v(\mathbf{y})$ is the phase velocity at the normal-incidence point, $\mathbf{D}(\mathbf{y})$ is the 2×2 curvature matrix of the reflector with respect to the local tangential coordinates also at the normal-incidence point and $\kappa_N = \kappa_N(\mathbf{x},\mathbf{y})$ is the KMAH index for the normal wave. Iversen (2006, equation 36) has derived the ray-propagator matrix for the reflected wave

$$\underline{\Pi}(\mathbf{x},\mathbf{y},\mathbf{x}) = \begin{pmatrix} 2(\mathbf{Q}_{NIP}\mathbf{P}_N^T + \mathbf{I})\mathbf{I}^* & 2\mathbf{Q}_{NIP}\mathbf{Q}_N^T\mathbf{I}^* \\ 2\mathbf{P}_{NIP}\mathbf{P}_N^T\mathbf{I}^* & (2\mathbf{P}_{NIP}\mathbf{Q}_N^T - \mathbf{I})\mathbf{I}^* \end{pmatrix} \tag{12}$$

where $\mathbf{Q}_{NIP} = \mathbf{Q}_{NIP}(\mathbf{x},\mathbf{y})$, $\mathbf{P}_{NIP} = \mathbf{P}_{NIP}(\mathbf{x},\mathbf{y})$, $\mathbf{I}$ is the identity matrix and $\mathbf{I}^* = \mathrm{diag}(1,-1)$. Comparison of equations 6 and 12, yields the important decomposition (Iversen, 2006, equation 48)

$$\mathbf{Q}_2(\mathbf{x},\mathbf{y},\mathbf{x}) = 2\mathbf{Q}_{NIP}(\mathbf{x},\mathbf{y})\mathbf{Q}_N^T(\mathbf{x},\mathbf{y})\mathbf{I}^*, \tag{13}$$

from which (Iversen, 2006, equations 49 and 60)

$$\mathscr{L}_R(\mathbf{x},\mathbf{y},\mathbf{x}) = 2\mathscr{L}_{NIP}(\mathbf{x},\mathbf{y})\mathscr{L}_N(\mathbf{x},\mathbf{y})\ . \tag{14}$$

and

$$\kappa_R(\mathbf{x},\mathbf{y},\mathbf{x}) = \kappa_{NIP}(\mathbf{x},\mathbf{y}) + \kappa_N(\mathbf{x},\mathbf{y}). \tag{15}$$

Combining equations 3, 7 and 10 with the two equations above and the reciprocity relation for the upward and downward transmission coefficients 4, gives the new decomposition formula

$$U_R(\mathbf{x},\mathbf{y},\mathbf{x};\omega) = U_{NIP}(\mathbf{x},\mathbf{y};\omega)\,U_N(\mathbf{x},\mathbf{y};\omega)/2\ . \tag{16}$$

The above decomposition shows that the amplitude response of the reflected wave is equal to the amplitude response of the NIP wave times the amplitude response of the normal wave divided by two.

Decomposition of the Green's function

The geometric ray approximation of the Green's function for the zero-offset reflected wave is (see, e.g., Červený, 2001, subsection 5.4.5 with a different notation)

$$G_{ij}^R(\mathbf{x},\mathbf{y},\mathbf{x};\omega) = \frac{h_i(\mathbf{x})\,U_R(\mathbf{x},\mathbf{y},\mathbf{x};\omega)\,h_j(\mathbf{x})}{4\pi\rho(\mathbf{x})v(\mathbf{x})}\ , \tag{17}$$

where $h_i(\mathbf{x})$ and $h_j(\mathbf{x})$ are the polarization vectors of the up- and down-going wave, respectively, $\rho(\mathbf{x})$ and $v(\mathbf{x})$ are the density and phase velocity at $\mathbf{x}$, and $U_R(\mathbf{x},\mathbf{y},\mathbf{x})$ is the amplitude given by equation 3.

The Green's function for the wave from the point-source, $\mathbf{x}$ at the surface to the normal-incidence-point, $\mathbf{y}$, at the reflector (the reverse NIP wave) is

$$G_{kj}^{NIP}(\mathbf{y},\mathbf{x};\omega) = \frac{h_k(\mathbf{y})\,U_{NIP}(\mathbf{y},\mathbf{x};\omega)\,h_j(\mathbf{x})}{4\pi[\rho(\mathbf{x})v(\mathbf{x})\rho(\mathbf{y})v(\mathbf{y})]^{1/2}}\ , \tag{18}$$

with analogous meanings for the quantities ρ, v, h_j and h_k and where $U_{NIP}(\mathbf{y},\mathbf{x};\omega)$ is given by equation 7. Note that the amplitude function is reciprocal, which allows us to interchange $\mathbf{x}$ and $\mathbf{y}$ in the expression for U_{NIP}.

The tensor response (not a proper Green's function) of the normal wave can be written

$$G_{ik}^N(\mathbf{x},\mathbf{y};\omega) = \frac{h_i(\mathbf{x})\,U_N(\mathbf{x},\mathbf{y};\omega)\,h_k(\mathbf{y})}{4\pi[\rho(\mathbf{x})v(\mathbf{x})\rho(\mathbf{y})v(\mathbf{y})]^{1/2}}\ , \tag{19}$$

where $U_N(\mathbf{y},\mathbf{x};\omega)$ is given by equation 10. Combining equations 17, 18 and 19 and taking into account equation 16, provides the decomposition formula

$$G_{ij}^R(\mathbf{x},\mathbf{y},\mathbf{x};\omega) = 2\pi\,\rho(\mathbf{y})\,v(\mathbf{y})\,G_{ik}^N(\mathbf{x},\mathbf{y};\omega)\,G_{kj}^{NIP}(\mathbf{y},\mathbf{x};\omega)\ , \tag{20}$$

where there is a summation over the index k.

The Green's function may also be expressed as a product of the Green's function from the surface to the reflection point times a factor that takes into account the reflector and times the Green's function from the reflector to the surface. For a normal-incidence reflected wave, this can be written (Schleicher et al., 2001)

$$G_{ij}(\mathbf{x},\mathbf{y},\mathbf{x};\omega) = 4\pi\,\rho(\mathbf{y})\,v(\mathbf{y})\,G_{ik}(\mathbf{x},\mathbf{y};\omega)\,G_{kj}(\mathbf{y},\mathbf{x};\omega)\,\frac{r_N\,e^{-i\frac{\pi}{2}\kappa_H}}{\mathscr{L}_H}\ , \tag{21}$$

where there again is a summation over k, and

$$\mathscr{L}_H = \frac{|\det\mathbf{H}|^{1/2}}{\cos\chi}\ , \tag{22}$$

with χ being the angle between the phase velocity (parallel to the reflector normal) and group velocity vectors. The matrix $\mathbf{H}$ is defined by

$$H_{ij} = 2\frac{\partial^2 T(\mathbf{y},\mathbf{x})}{\partial\sigma_i\partial\sigma_j} \ , \tag{23}$$

where σ_i, $i = 1,2$, are Cartesian coordinates on the tangent plane to the reflector at the normal-incident point, $\mathbf{y}$, taken as the origin. The contribution to the KMAH index is

$$\kappa_H = 1 - \mathrm{Sgn}(\mathbf{H})/2 \ , \tag{24}$$

where $\mathrm{Sgn}(\mathbf{H})$ is the signature of the (symmetric) matrix $\mathbf{H}$, which is equal to number of positive eigenvalues minus the number of negative eigenvalues. We assume the matrix $\mathbf{H}$ to be nonsingular, namely, $\det\mathbf{H} \neq 0$.

Comparison of equations 20 and 21 gives (see Iversen, 2006, equations 54 and 61)

$$\mathscr{L}_N = \mathscr{L}_{NIP}\mathscr{L}_H/2 \quad \text{and} \quad \kappa_N = \kappa_{NIP} + \kappa_H \ . \tag{25}$$

This shows that the normal wave incorporates the influence of the reflector on the reflected wave.

True Amplitude Depth Migration

We consider the depth migration of PP or SS zero-offset primary reflections under the assumption of a smooth background model. Moreover, we also assume that, by adequate preprocessing, multiples have been attenuated or removed and that, in the frequency domain, primary reflections are reasonably represented as in equation 3. In other words, the input zero-offset section approximately consists of a superposition of primaries, other events being considered as noise.

A discussion on the available approaches to obtain a reliable zero-offset (stacked) section to implement the migration procedures described below is beyond the scope of the present paper. In this way, we assume that the data have been reduced to a scalar recording of PP or SS primary reflections, and that an adequate depth macro-model is already available.

Based on the geometrical-spreading and KMAH decomposition formulas 14 and 15, we can devise the following three schemes for true-amplitude zero-offset migration. The first scheme consists of map migration of selected reflectors (see, e.g., Kleyn, 1977, Gjøystdal and Ursin, 1981 and Gjøystdal et al., 1984) in which true amplitudes (i.e., amplitudes corrected for geometrical spreading) are attached. The second method is a pre-stack depth migration based on ray tracing, like Kirchhoff migration (Hubral et al, 1991) or inverse generalized Radon Transform (Ursin, 2004). Finally, the recorded wavefield may be downward continued in a half-velocity model (Loewenthal, 1976; Gazdag and Sguazzero, 1984). This requires an additional geometrical-spreading correction. A quick description of the different algorithms is given below.

True-amplitude map migration

For a given reflector, we consider that the zero-offset, normal-incidence traveltime, $T_R(\mathbf{x})$, as well as its amplitude, $U_R(\mathbf{x};\omega)$, have been estimated from the data. The slowness vector, $\mathbf{p}(\mathbf{x})$, at any ZO trace location, $\mathbf{x}$, can be estimated by the first traveltime derivatives

$$p_k(\mathbf{x}) = \frac{\partial T_R(\mathbf{x})}{\partial x_k} \ . \tag{26}$$

This provides the initial values for the normal-incidence rays, which are traced downwards to half the total traveltime, $T(\mathbf{y},\mathbf{x}) = T_R(\mathbf{x})/2$. The points $\mathbf{y}$ define the reflector. The second derivatives of traveltime,

$$B_{jk}(\mathbf{x}) = \frac{\partial^2 T_R(\mathbf{x})}{\partial x_j\partial x_k} \ , \tag{27}$$

may be used to downward continue the curvature of the normal wave. This gives us an estimate of the curvature matrix, $\mathbf{D}(\mathbf{y})$, of the reflector (Gjøystdal et al., 1984). An interpolation scheme must then be used to construct the reflecting interface, $y_3 = \phi(y_1,y_2)$. In the ray tracing from $\mathbf{x}$ to $\mathbf{y}$ along the normal-incidence ray, the geometrical-spreading factors for the NIP-wave, $\mathscr{L}_{NIP}(\mathbf{y},\mathbf{x})$ and the normal wave, $\mathscr{L}_N(\mathbf{y},\mathbf{x})$, as well as the corresponding KMAH indexes, $\kappa_{NIP}(\mathbf{y},\mathbf{x})$ and $\kappa_N(\mathbf{y},\mathbf{x})$, have been computed. Assuming that the product of transmission coefficients is close to one, an estimate of the normal-incidence reflection coefficient at the depth point $\mathbf{y}$ is

$$\begin{aligned} r_N(\mathbf{y}) \quad &= \quad 2\mathscr{L}_{NIP}(\mathbf{y},\mathbf{x})\mathscr{L}_N(\mathbf{y},\mathbf{x})e^{i\frac{\pi}{2}(\kappa_{NIP}(\mathbf{y},\mathbf{x})+\kappa_N(\mathbf{y},\mathbf{x}))} \\ &\times \quad \left\{\frac{1}{\pi}\int_0^\infty U_R(\mathbf{x};\omega)\,e^{-i\omega T_R(\mathbf{x})}\,d\omega\right\} \ , \end{aligned} \tag{28}$$

Note that the picked traveltime, $T_R(\mathbf{x})$, represents the traveltime, $T_R(\mathbf{x},\mathbf{y},\mathbf{x})$, that appears in equation 3.

Ray-based depth migration

A general form of a post-stack depth migration integral based on ray tracing is the Kirchhoff or diffraction stack migration. For a depth point, $\mathbf{y}$, at a reflector, an estimate of the normal-incidence reflection coefficient, $r_N(\mathbf{y})$, is given by

$$r_N(\mathbf{y}) = \frac{1}{2\pi^2}\int_0^\infty d\omega\, i\omega \int_\Sigma d\mathbf{x}\, U_R(\mathbf{x};\omega)\, w(\mathbf{y},\mathbf{x})e^{-i[2\omega T(\mathbf{y},\mathbf{x})-\kappa_{NIP}(\mathbf{x},\mathbf{y})]} \tag{29}$$

where $U_R(\mathbf{x};\omega)$ is the recorded data in the frequency domain, $T(\mathbf{y},\mathbf{x})$, is the one-way traveltime along the ray from the surface point, $\mathbf{x}$, to the image point, $\mathbf{y}$, and $\kappa_{NIP}(\mathbf{y},\mathbf{x})$ is the KMAH index and $w(\mathbf{y},\mathbf{x})$ is a true-amplitude weight. The integration is performed over all or part of the data acquisition surface, Σ.

If the reflector dip is known, we can use equation 71 in Ursin (2004), together with equation 4.34 in Burridge et al. (1998), to derive the true-amplitude weight function

$$w(\mathbf{y},\mathbf{x}) = 4\,\frac{\cos\alpha(\mathbf{x})}{\cos\chi(\mathbf{x})}\,\frac{\cos\chi(\mathbf{y})}{\cos\alpha(\mathbf{y})} \ . \tag{30}$$

Here, $\alpha(\mathbf{x})$ is the angle (group velocity) the ray makes with the recording surface at $\mathbf{x}$ and $\chi(\mathbf{x})$ is the angle between phase and group velocity at $\mathbf{x}$. Also, $\alpha(\mathbf{y})$ is the angle the ray (group velocity) and the normal at the reflecting surface at $\mathbf{y}$, and $\chi(\mathbf{y})$ is the angle between phase and group velocity at $\mathbf{y}$.

We observe that, when the ray from $\mathbf{x}$ to $\mathbf{y}$ is a normal-incidence ray, namely when $\mathbf{x}$ is the stationary point associated with $\mathbf{y}$, the angles $\alpha(\mathbf{y})$ and $\chi(\mathbf{y})$ coincide. As a consequence, the true-amplitude weight 30 reduces to the simpler, dip-independent expression

$$w(\mathbf{y},\mathbf{x}) = 4\,\frac{\cos\alpha(\mathbf{x})}{\cos\chi(\mathbf{x})} \ . \tag{31}$$

If the geological dip is unknown, we may approximate expression 30 by expression 31 to obtain a true-amplitude Kirchhoff migration that does not depend on the reflector dip. The asymptotic evaluation of the Kirchhoff integral in equation 29, using the amplitude weights 30 or 31, produces the same result. Equation 31 represents a natural extension to anisotropic media of the corresponding expression for isotropic media, as given in Schleicher et al. (1993).

Wave-equation continuation

The true-amplitude Kirchhoff migration algorithm described above may have problems in complex geology with many caustics and traveltime triplications. Then a wave-equation continuation may be used.

In the exploding reflector model for seismic migration, it is assumed that the preprocessed seismic data, $u_R(\mathbf{x},t)$, is the upgoing wavefield. The Fourier transform of the data, $U_R(\mathbf{x},\omega)$, are reverse propagated in a half-velocity model. In anisotropic media this is obtained by multiplying the density by two and dividing the elastic parameters by two (see Appendix). The migration can be understood as reverse-propagating the normal wave, so that, as a consequence, only the normal-wave part of the geometrical spreading for the reflected wave is compensated. The image at depth is taken for time equal zero. At any reflector point, $\mathbf{y}$, the migration result is approximately

$$I_R(\mathbf{y}) = \frac{r_N(\mathbf{y})\, e^{-i\frac{\pi}{2}\kappa_{NIP}(\mathbf{y},\mathbf{x})}}{2\mathscr{L}_{NIP}(\mathbf{y},\mathbf{x})}\ , \tag{32}$$

where $\mathbf{x}$ is the point where the normal ray from $\mathbf{y}$ hits the measurement surface.

In order to estimate and correct for the geometrical-spreading factor, $\mathscr{L}_{NIP}(\mathbf{y},\mathbf{x})$, and KMAH index, $\kappa_{NIP}(\mathbf{y},\mathbf{x})$, we must know the geological dip. Then we can compute these quantities by tracing the normal-incidence ray, starting at the image point, $\mathbf{y}$, normal to the geological dip, up to the emergence point, $\mathbf{x}$, at the data acquisition surface.

If this is not possible, we may perform an additional Kirchhoff migration, this time with the new weight

$$w_1(\mathbf{y},\mathbf{x}) = w(\mathbf{y},\mathbf{x})[2\mathscr{L}_{NIP}(\mathbf{y},\mathbf{x})\, e^{i\frac{\pi}{2}\kappa_{NIP}(\mathbf{y},\mathbf{x})}]\ . \tag{33}$$

The resulting amplitude at depth is approximately given by

$$I_K(\mathbf{y}) = r_N(\mathbf{y})[2\mathscr{L}_{NIP}(\mathbf{y},\mathbf{x})\, e^{i\frac{\pi}{2}\kappa_{NIP}(\mathbf{y},\mathbf{x})}]\ . \tag{34}$$

Combination of equations 32 and 34 permits us to define the quantity

$$C(\mathbf{y}) = 2\mathscr{L}_{NIP}(\mathbf{y},\mathbf{x})e^{i\frac{\pi}{2}\kappa_{NIP}(\mathbf{y},\mathbf{x})} = \frac{I_R(\mathbf{y})}{I_K(\mathbf{y})}\ . \tag{35}$$

After smoothing, this quantity is used as a correction factor applied to the previous migrated data of equation 32, leading to an estimate of the normal-incidence reflection coefficient

$$r_N(\mathbf{y}) = I_R(\mathbf{y})C(\mathbf{y})\ . \tag{36}$$

CONCLUSIONS

We have shown that the ray theoretical Green's tensor for the normal-incidence reflected wave is equal to the product of a constant times the tensor response of the normal wave times the Green's tensor of the reverse NIP wave. Using the normal wave resulted in a scheme for true-amplitude map migration. True-amplitude post-stack depth migration can be done by a ray-based migration algorithm or reverse-propagating the recorded wavefield in a model with half the elastic constants and double the density. This results in a half-velocity model in anisotropic media. The image is formed by taking the reverse-propagated wavefield at time equal zero followed by an additional geometrical spreading correction.

ACKNOWLEDGEMENTS

We want to thank Einar Iversen for helpful discussions. M. Tygel acknowledges support from the *National Council of Scientific and Technological Development (CNPq)*, Brazil, the *Research Foundation of the State of São Paulo (FAPESP)*, Brazil, and the sponsors of the *Wave Inversion Technology (WIT) Consortium*, Germany. B. Ursin acknowledges support from *Statoil* and the *Norwegian Council of Research* via the ROSE project.

References

Bleistein, N., 1987, On the imaging of reflectors in the Earth: Geophysics, **52**, 931–942.

Burridge, R., M. de Hoop, D. Miller, and C. Spencer, 1998, Multiparameter inversion in anisotropic media: Geophysical Journal International, **134**, 757–777.

Červený, V., 2001, Seismic ray theory: Cambridge University Press.

Chapman, C. H., 1994, Reflection/transmission reciprocities in anisotropic media: Geophysical Journal International, **116**, 498–501.

———, 2004, Fundamentals of seismic wave propagation: Cambridge University Press.

Chernyak, V. S. and S. A. Gritsenko, 1979, Interpretation of effective common depth point parameters for a spatial system of homogeneous beds with curved boundaries: Soviet Geology and Geophysics, **20**, 91–98.

Gazdag, J. and P. Sguazzero, 1984, Migration of seismic data: IEEE Proceedings, **72**, 1302–1315.

Gjøystdal, H., J. E. Reinhardsen, and B. Ursin, 1984, Traveltime and wavefront curvature calculations in three-dimensional inhomogeneous layered media with curved interfaces: Geophysics, **49**, 1466–1494.

Gjøystdal, H. and B. Ursin, 1981, Inversion of reflection times in three-dimensions: Geophysics, **46**, 972–983.

Hubral, P., 1983, Computing true amplitude reflections in a laterally inhomogeneous earth: Geophysics, **48**, 1051–1062.

Iversen, E., 2006, Amplitude, Fresnel zone and NMO velocity for PP and SS normal-incidence reflections: Geophysics, **71**, W1 – W14.

Kleyn, A. H., 1977, On the migration of reflection-time contour maps: Geophysical Prospecting, **25**, 125–140.

Krey, T., 1976, Computation of interval velocities from common-reflection-point moveout times for n-layers with arbitrary dips and curvatures in three dimensions when assuming small shot-geophone distances: Geophysical Prospecting, **24**, 91–111.

Loewenthal, D., L. Lu, R. Roberson, and J. Sherwood, 1976, The wave equation applied to migration: Geophysical Prospecting, **24**, 380–399.

Schleicher, J., M. Tygel, and P. Hubral, 1993, 3-D true-amplitude finite-offset migration: Geophysics, **58**, 1112–1126.

Schleicher, J., M. Tygel, B. Ursin, and N. Bleistein, 2001, The Kirchhoff-Helmholtz integral for anisotropic elastic media: Wave Motion, **34**, 353–364.

Tygel, M., J. Schleicher, P. Hubral, and C. Hanitzsch, 1993, Multiple weights in diffraction stack migration: Geophysics, **58**, 1820–1830.

Ursin, B., 1982, Quadratic wavefront and traveltime approximations in homogeneous layered media with curved interfaces: Geophysics, **47**, 1012–1021.

———, 2004, Parameter inversion and angle migration in anisotropic elastic media: Geophysics, **69**, 1125–1142.

Appendix A: Construction of an anisotropic half-velocity model

In this appendix, we explain how to modify the parameters of a given anisotropic medium so that the velocities in the new medium equal the corresponding ones of the original medium, multiplied by a user selected constant. In particular, we use this strategy to construct the "half-velocity model" needed for the post-stack migration scheme used in the main text.

We adopt the notation and basics of anisotropic wave propagation from Chapman (2004). We consider a given anisotropic medium specified by the density-normalized matrices

$$\mathbf{a}_{ij} = \mathbf{c}_{ij}/\rho \ , \tag{A-1}$$

where $(\mathbf{c}_{ij})_{kl} = c_{ijkl}$ is the elastic-parameter tensor in contracted notation and ρ is the density function. A explained in, e.g., (Červený, 2001, section 2.2.4), for a given direction vector, $\hat{\mathbf{p}} = (\hat{p}_i)$, the associated Christoffel matrix, Γ, is defined by

$$\Gamma = \hat{p}_i \hat{p}_j \mathbf{a}_{jk} \ , \tag{A-2}$$

for which the associated eigen-equation is

$$\left(v^2 \mathbf{I} - \Gamma\right) \hat{\mathbf{g}} = \mathbf{0} \ . \tag{A-3}$$

The three eigenvalues, v, (namely, $v = v_I$, with $I = 1,2,3$), are the phase velocities of three different wave modes, which determine the corresponding permitted slowness vectors $\mathbf{p} = \hat{\mathbf{p}}/v$. The corresponding (unit) eigenvectors, $\hat{\mathbf{g}}$, are the polarization vectors.

We consider the equations of motion and constitutive relations of wave propagation in an anisotropic medium, as given in Chapman (2004), equations (4.5.35) and (4.5.36), with a slightly different notation

$$\frac{\partial \mathbf{w}}{\partial t} = \frac{1}{\rho} \frac{\partial \mathbf{t}_j}{\partial x_j} + \frac{1}{\rho} \mathbf{f} \quad \text{and} \quad \frac{\partial \mathbf{t}_j}{\partial t} = \mathbf{c}_{jk} \frac{\partial \mathbf{w}}{\partial x_k} \ . \tag{A-4}$$

In the above equations, $\mathbf{w}$, denotes the particle velocity vector (as opposed to Chapman that uses $\mathbf{v}$ for that quantity) and $\mathbf{t}_j$ is the j-th component (column) of the stress tensor. If we divide equations A-4 by a scalar, $K \neq 0$, and then change variables

$$t \to t' = Kt, \quad \rho \to \rho' = K\rho \quad \text{and} \quad \mathbf{c}_{ij} \to \mathbf{c}'_{ij} = \mathbf{c}_{ij}/K \ , \tag{A-5}$$

we see that the new equations are of the same form as the old ones. In particular, the new Christoffel equation reads

$$\left((v')^2 \mathbf{I} - \Gamma'\right) \hat{\mathbf{g}}' = \mathbf{0} \ , \tag{A-6}$$

where v', Γ' and $\hat{\mathbf{g}}'$ are the modified quantities that correspond to v, Γ and $\hat{\mathbf{g}}$, respectively, after the change of variables. From equations A-1, A-2 and A-5, we see that

$$\mathbf{a}'_{ij} = (1/K^2)\mathbf{a}_{ij} \quad \text{and} \quad \Gamma' = (1/K^2)\Gamma \ . \tag{A-7}$$

Substitution into equation A-6 yields

$$\left((K v')^2 \mathbf{I} - \Gamma\right) \hat{\mathbf{g}}' = \mathbf{0} \ , \tag{A-8}$$

which has the solutions

$$v' = v/K \quad \text{and} \quad \hat{\mathbf{g}}' = \hat{\mathbf{g}} \ . \tag{A-9}$$

The new slowness vector, $\mathbf{p}'$ and group velocity vector, $\mathbf{V}'$, satisfy

$$\mathbf{p}' = \frac{1}{v'} \hat{\mathbf{p}} = \frac{1}{(v/K)} \hat{\mathbf{p}} = K\mathbf{p} \ . \tag{A-10}$$

and

$$V'_i = a'_{ijkl}\, p'_k\, \hat{g}_j\, \hat{g}_l = \frac{a_{ijkl}}{K^2}\,(K p_k)\, \hat{g}_j\, \hat{g}_l \ = V_i/K. \tag{A-11}$$

Equations A-9 and A-11 tell us that the phase and group velocity are both scaled by $1/K$ in the new medium. This is what we expected since the equations of motion and constitutive relations A-4 remained unchanged for the new elastic parameter tensor and new density, together with the fact that the new time has been multiplied by K (see equation A-5). From this we see that, to obtain a half-velocity model, one has to divide the elastic parameter tensor by two and multiply the density by two.